DESIGN, FABRICATION AND EXPERIMENTAL STUDY OF A FLAT PLATE COLLECTOR SIMULATOR

O. R. S. Rodríguez[a], R. N. N. Koury[b], and A. A. T. Maia[b]

[a]Universidade Federal de Minas Gerais
Departamento de Pós-graduação em Engenharia Mecânica
Av. Pres. Antônio Carlos, 6627 - Pampulha
Belo Horizonte - MG, 31270-901, Brasil
ingpino@ufmg.br

[b]Universidade Federal de Minas Gerais
Departamento de Engenharia Mecânica
Av. Pres. Antônio Carlos, 6627 - Pampulha
Belo Horizonte - MG, 31270-901, Brasil
koury@demec.ufmg.br

Received: April 02, 2016
Revised: May 10, 2016
Accepted: June 14, 2016

ABSTRACT

In this article, a flat plate collector simulator was designed and developed based on the use of electric heaters and a power control system. A computational algorithm aimed at determining the relationship between the incident solar energy on the collector absorber plate and the corresponding amount of power that must be supplied by the electrical resistance was developed. The variation in power is obtained by regulating the voltage fed through the assembly. With such regulation, simulating typical profiles of insolation over a day was possible. In the assessment of the average solar radiation data obtained by satellite imagery analysis (SWERA Project), the results showed that the thermal behavior of the simulator collector was close with a real behavior. Therefore, it can be used to determine the operating characteristics of auxiliary power systems as heat pumps, electrical systems or water heating systems. Different thermodynamic processes to determine the main losses of a collector evaluated the simulation parameters.

Keywords: simulation, water heating, fabrication, solar collector

NOMENCLATURE

A	area, elevation, m² or m
C_p	specific heat, $kJkg^{-1}K^{-1}$
e	emissive power, Wm^{-2}
F_R	heat removal factor
f	modulation factor
G_{sc}	solar constant, Wm^{-2}
h_w	heat transfer coefficient for the wind,$Wm^{-2}K$
I	hourly radiation, MJm^{-2}
I_R	refractive index
K	extinction coefficient, m^{-1}
k	thermal conductivity, $Wm^{-2}K^{-1}$
KT,kt	clarity index
L	length, m
$\dot{m}$	mass flow, kgs^{-1}
n	day for the year
N	number glass covers, number of hours
P	power, perimeter, W or m
Q	heat rate, W
r	reflectivity
R	resistance, Ω
R_B	direct radiation rate on the inclined plane
S	Solar radiation absorbed, MJm^{-2}
t	time, thickness, s or m
T	temperature, K
U_b	energy losses in the collector base, W
U_e	energy losses on the side of the collector, W
U_L	energy losses on the upper surface of the collector, W
U_T	total energy losses in the collector, W
V	voltage, V
Z	constant programming

Greek symbols

α	absorptance or absorption power
β	slope
δ	declination
ε	emittance, $Wm^{-2}m^{-1}$
θ	angle between surface normal and incident radiation
ρ	reflectance
τ	transmittance
σ	Stefan-Boltzmann constant
φ	latitude
ω	hour angle

Subscripts

1	after hour
2	before hour
a	ambient, absorbed
b	direct
c	collector
d	beam
f	fluid

g ground
i input
l lateral
m average
n normal
o output, global
p plate
r radiation
T on an inclined plane
u useful
w water
x for d, g and b
⊥ Perpendicular
‖ Parallel

INTRODUCTION

The growth in the human population, as well as the access to better life conditions, is making energetic demand to be bigger every day. In the last years, however, concerns have been growing due to two factors: the environmental impacts of burning large amounts of fossil fuels and the lack of knowledge regarding meeting the growing demand on current global reserves. Driven by these facts, NGOs are working to increase the contribution of renewable energy sources and, therefore, reduce the consumption of such fuels, which will contribute to reduce the problems mentioned before (Ibrahim et al., 2014). On the other hand, a significant share of the total energy produced in the world is used for domestic water heating, that share being 11% in the United States of America (Levine et al., 2007), 14% in Europe (ADEME, 2009), 24% in Brazil (Dos Santos et al., 2011) and 27% in China (Zhou et al., 2008).

As a way of reducing this consumption in Brazil and also contributing to the use of alternative energy sources, devices that use solar energy in order to heat water for domestic purposes are being used (Sandoval et al., 2014). However, a restriction to the use of these systems alone is the lack of sunny days throughout the year. Due to this issue, this article designs, builds and discusses the experimental results obtained in a low cost device with the intent of simulating a solar collector and, by doing so, aiding future researches in the characterization of auxiliary systems.

DESIGN AND FABRICATION

The design and features of the solar collector simulator are illustrated in Fig. 1, and includes the computational software, a solar collector simulator, an electronic control together with the electric resistances, an isolation system for each component and a water storage tank (Sandoval, 2015). During the operation, a connection between the simulating equipment and the computational software developed to do the data processing is used. This computational algorithm acquires and transfers the daily solar data and the power that must be applied to the water in order to obtain an equivalent heating when compared to the solar radiation absorbed by a configured solar collector. The methodology and correlations used in this article are described by authors Duffie and Beckman (2013).

Mathematical Equations

The development of the computational algorithm was done with the intent of using solar radiation databases:

The solar declination (δ),

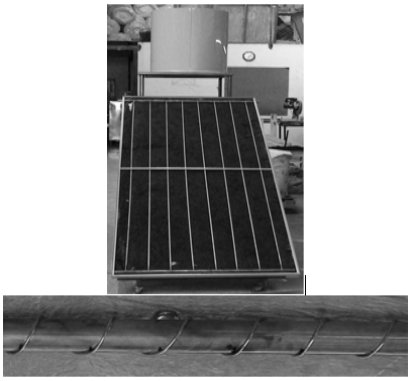

Figure 1. Solar simulated system design.

$$\delta = 23.45°\sin\left(360\frac{284+n}{365}\right) \quad (1)$$

can be calculated through Eq. (1) (Cooper, 1969).

$$\omega_1 = 15(Z-1)-120 \quad (2)$$

$$\omega_2 = 15Z-120 \quad (3)$$

$$\omega = \omega_1 + 7.5 \quad (4)$$

The hour angles and average hour angle are calculated through Eq. (2), (3) and (4), where Z=1 when it is 4h (Sandoval, 2015).

$$I_o = \left(\frac{43000}{\pi}\right) + G_{SC}\left[1+0.033\cos\left(\frac{360n}{365}\right)\right] \{\cos(\varphi)\cos(\delta)[\sin(\omega_2)-\sin(\omega_1)]\} + \left[\frac{\pi(\omega_2-\omega_1)}{180}\right]\sin(\varphi)\sin(\delta) \quad (5)$$

$$k_T = I/I_o \quad (6)$$

The equation (6) provides the calculation of the cloud distribution coefficient for a clear sky and a cloudy sky day for the solar radiation (Liu and Jordan, 1960), for to know this value, it´s necessary to solve the Eq. (5).

$$I_d/I = 1 - 0.09k_T \text{ for } k_T \leq 0.22 \quad (7)$$

$$I_d/I = 0.9511 - 0.1604k_T + 4.388k_T^2 - 16.638k_T^3 + 12.366k_T^4 \text{ for } 0.22 < k_T \geq 0.8 \quad (8)$$

$$I_d/I = 0.165 \text{ for } k_T > 0.8 \quad (9)$$

The calculation of the components for the hour solar radiation can be obtained through Eq. (7), (8) and (9) in each case. The fraction of diffuse radiation is defined by the correlation of Erbs, Klein and Duffie (1982).

$$R_b = \frac{\cos(\varphi+\beta)\cos(\delta)\cos(\omega) + \sin(\varphi+\beta)\sin(\delta)}{\cos(\varphi)\cos(\delta)\cos(\omega) + \sin(\varphi)\sin(\delta)} \quad (10)$$

The fraction of direct solar radiation can be obtained by subtracting the diffuse radiation fraction from the global radiation. For the calculation of the proportion of the direct radiation in an inclined plane (usually horizontal), Eq. (10) is used.

$$\theta_{1b} = \cos^{-1}[\cos(\varphi+\beta)\cos(\delta)\cos(\omega) + \sin(\varphi+\beta)\sin(\delta)] \quad (11)$$

$$\theta_{1g} = 90 - 0.5788\beta + 0.002693\beta^2 \quad (12)$$

$$\theta_{1d} = 59.7 - 0.1388\beta + 0.001497\beta^2 \quad (13)$$

$$I_R = \frac{\sin(\theta_{1x})}{\sin(\theta_{2x})} \quad (14)$$

One can notice that this correlation relies on the local factors, the panel inclination and the average hour angle evaluated. After having determined the solar radiation parameters, a calculation for the solar radiation absorbed in the collector must be done for each hour. In order to do this, the values of the radiation reflection indexes must be known. The calculation of the external and internal angles of incidence in the glass for the direct, diffuse and albedo radiation are obtained from Eq. (11), (12), (13) and (14) respectively, knowing that the reflectance index for common glass is 1,526 (Duffie and Beckman, 2013). The angles vary according the solar collector inclination in respect to the ground. Where x represents the possibility of using the equation in order to determine the index for the three components.

After having determined the incidence angles, the perpendicular and the parallel components of the non-polarized radiation must be evaluated and have their mean values calculated.

$$r_\perp = \frac{\sin^2(\theta_{2x} - \theta_{1x})}{\sin^2(\theta_{2x} + \theta_{1x})} \quad (15)$$

$$r_\parallel = \frac{\tan^2(\theta_{2x} - \theta_{1x})}{\tan^2(\theta_{2x} + \theta_{1x})} \quad (16)$$

$$r = \frac{(r_\perp + r_\parallel)}{2} \quad (17)$$

$$\tau_r = \frac{1}{2}\left(\frac{1-r_\parallel}{1+r_\parallel} + \frac{1-r_\perp}{1+r_\perp}\right) \quad (18)$$

For smooth surfaces, Fresnel suggests using Eq. (15), (16) and (17) for the reflection of the non-polarized radiation going from surface one to surface two (Duffie and Beckman, 2013).

$$\tau_a = e^{\left[\frac{KL}{\cos(\theta_{2x})}\right]} \quad (19)$$

The absorption of the radiation in a partially transparent surface is described by Bouguer's law (Duffie and Beckman, 2013), Eq. (19), which is based on the hypothesis that the absorbed radiation is proportional to the intensity of the radiation in the surface and the distance (x) travelled by the radiation through the surface.

Where K ranges from 4 m^{-1} for commonly used glasses to 32 m^{-1} for glasses with a high amount of iron oxide; and L is the thickness of the glass, assumed to have a standard value of 3 mm in this paper.

$$\tau = \tau_a \frac{1-r_\perp}{1+r_\perp}\left[\frac{1-r_\perp^2}{1-(r_\perp\tau_a)^2}\right] \quad (20)$$

$$\rho = r_\perp(1+\tau_a\tau) \quad (21)$$

$$\alpha = (1-\tau_a)\left[\frac{1-r_\perp}{1-r_\perp\tau_a}\right] \quad (22)$$

The transmittance, reflectance and absorbance for a simple absorbent covers are evaluated with the help of Eq. (20), (21) and (22), and can be determined including the system losses with the method described by Siegel and Howell (2002).

$$\frac{\alpha}{\alpha_n} = 1 + 1.5879\cdot10^{-3}\theta + 2.7314\cdot10^{-4}\theta^2 - 2.3026\cdot10^{-5}\theta^3 + 9.0244\cdot10^{-7}\theta^4 - 1.8\cdot10^{-8}\theta^5 + 1.7734\cdot10^{-10}\theta^6 - 6.9937\cdot10^{-13}\theta^7 \quad (23)$$

The Pettit and Sowell (1976) polynomial, described in Eq. (23), is used for determining the direction of the absorbance for the solar radiation in a dark surface of an ordinary plate. This polynomial is a function of the incidence angle of the radiation on the surface.

$$(\tau\alpha)_x = 1.01\tau(\alpha/\alpha_n)\alpha_n \quad (24)$$

The transmittance-absorbance product, Eq. (24), must be thought of as a property of a combination of absorbent covers, instead of the product of two properties:

$$S = I_b R_b (\tau\alpha)_b + I_d (\tau\alpha)_d \left[\frac{1+\cos(\beta)}{2}\right] + \rho_g I_T (\tau\alpha)_g \left[\frac{1-\cos(\beta)}{2}\right] \quad (25)$$

Lastly, the calculations for determining the power absorbed by the plate, described by Eq. (25), are done. This power is called S. In order to obtain the value of the power S one must know the data needed by the aforementioned equations, from the radiation reflection to the transmittance-absorbance product.

$$U_T = \left\{\frac{N}{\frac{C}{T_{pm}}\left[\frac{T_{pm}-T_a}{N+f}\right]^e} + \frac{1}{h_W}\right\}^{-1} + \frac{\sigma\left(T_{pm}+T_a\right)\left(T_{pm}^2+T_a^2\right)}{\frac{1}{\varepsilon_p + 0.00591Nh_W} + \frac{2N+f-1+0.133\varepsilon_p}{\varepsilon_g} - N} \quad (26)$$

$$f = \left(1 + 0.089h_W - 0.1166h_W\varepsilon_p\right)\left(1 + 0.07866N\right) \quad (27)$$

$$C = 520\left(1 - 0.000051\beta^2\right) \quad (28)$$

$$e = 0.430\left(1 - \frac{100}{T_{pm}}\right) \quad (29)$$

$$U_b = k/L \quad (30)$$

$$U_e = (UA)_l / A_c \quad (31)$$

$$(UA)_l = (k/t_l) P_c t_c \quad (32)$$

$$U_L = U_b + U_c + U_T \quad (33)$$

From the values calculated through Eq. (26), (27), (28), (29), (30), (31) e (32), it is possible to calculate the total losses in the collector using Eq. (33).

Equation (26) makes the evaluation of the heat losses on the upper surface of the collector possible. Eq. (30) is used for determining the heat losses in the lower surface of the collector and Eq. (31) calculates the losses in the lateral surfaces.

In most collectors, the evaluation of the heat losses in the lateral surface is complex. However, in a well-designed system, these losses can be so small that there is no need for calculating them with great precision. Tabor (1959) recommends using a lateral insulation as wide as the collector's lower surface. These losses are evaluated assuming a one-dimensional heat flow in the collector's entire perimeter:

$$Q_u = A_c F_R \left[S - U_L\left(T_i - T_a\right)\right] \quad (34)$$

$$F_R = \frac{\dot{m}C_p}{A_c U_L}\left[\frac{\frac{S}{U_L}\left(T_{fo}-T_a\right)}{\frac{S}{U_L}\left(T_{fi}-T_a\right)}\right] \quad (35)$$

The final heat that must be transmitted to the water is determined through Eq. (34). This is the amount of heat that the resistances must generate. In order to make this possible, the water inlet temperature and the ambient temperature must be constantly measured. Where factor F_R is the collector plate removal factor and is calculated with the aid of Eq. (35).

$$P = 450Q_u \quad (36)$$

$$V = \sqrt{\frac{P}{R}} \quad (37)$$

Knowing the theoretical value of the heat that must be transmitted to the water, such value must be converted to the heating coming from the electric power. Therefore, the last calculations in the algorithm are: the value of the electric power obtained from Eq. (36) and the voltage value calculated through Eq. (37).

Lastly, the calculation of these variables is done for all the hourly radiation data stored in a day of evaluation.

Design of the Simulated Collector

In order to do the calculations and provide the necessary data for the thermodynamic modeling of a collector, Tab. 1 provides the necessary characteristics of a standard collector.

Table 1. Parameters of the simulated collector.

Parameter	Value
Area of the collector	2.4 m²
Number of covers	1
Thickness of the covering glass	3 mm
Inclination of the collector	36°
Average refractance index for glass – 1 cover	1.526
Emittance of the dark painted plate	0.96
Emittance of the glass	0.88
Thickness of the lateral insulation	25 mm
Thickness of the plate insulation	50 mm
Conductivity of the insulator	0.045 W/m °C
Amount of tubes	8
Diameter of the tubes	10 mm
Distance between tubes	12 mm
Conductivity of the plate	385 W/m °C
Thickness of the plate	0.5 mm

Fabrication Materials

The electric resistances are made of a Kanthal Nickel-Chromium wire with the following properties: Diameter 0.912mm, composition 80% Nickel and 20% Chromium, resistivity 1.6685 Ω\m and working temperature up to 1200°C.

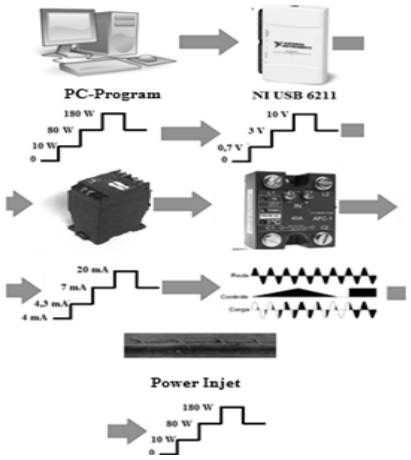

Figure 2. Illustration of the control for activating the simulating resistance.

In the modulation of the electric power (Fig. 2), an analogic exit, a signal conversion module and a solid state relay for controlling the voltage through the phase angle were needed. When combined, these devices allow for the modulation of the power supply. This way, the electric resistances in the interior of the solar collector can dissipate different amounts of heat with the intent of simulating the solar radiation in a specific time of the day. The simulation of different radiation behaviors makes it possible to raise the water temperatures.

RESULTS AND DISCUSSION

Test Methodology

In order to compare results, the following test was done on the system: water heating through the collector simulating the seasonal radiations that are representative for the city of Belo Horizonte - MG.

For each of the above mentioned situations, the following data were obtained:

1. Ambient temperature;
2. Temperature of the water in the collector (measured in five different points);
3. Temperature of the water in the storage tank.

This methodology has the intent of characterizing the system behavior under real solar radiation conditions.

Result and analysis

The evaluation of the data acquired from the Radiasol® (Labsol, 2014) software made it possible to illustrate, in Fig. 3, the behavior of the monthly average hourly horizontal radiation reaching the region of Belo Horizonte and also apply the values for such radiation in the computational algorithm, allowing for, in Fig. 5, plotting the average contributions of solar radiation.

The behaviors are illustrated as following:

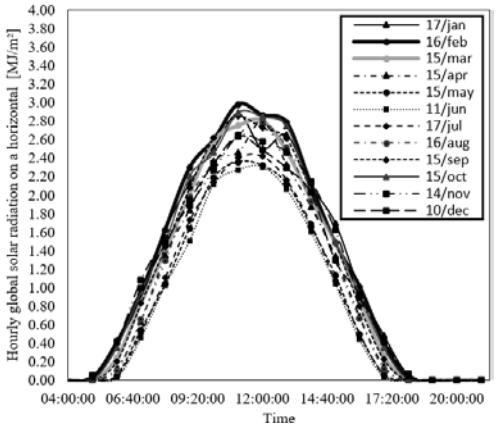

Figure 3. Monthly average hourly horizontal radiation.

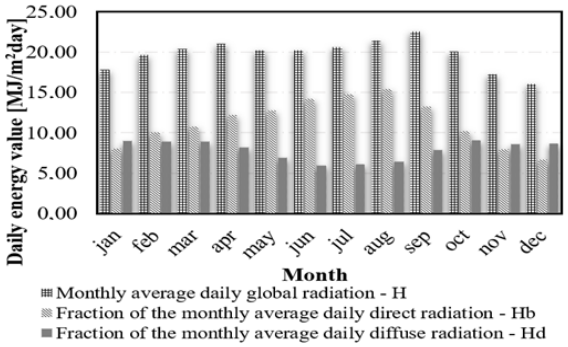

Figure 4. Global radiation, diffuse fraction and direct fraction of the monthly average daily direct radiation.

The values of the monthly average clarity index were used in the evaluation of the implemented mathematical models, because it made it possible to compare with values found in the literature. The compared values were the ondes found in the solarimetric atlas of Minas Gerais (Cemig, 2011) and in the SUNDATA (Censolar, 1993) database.

By analyzing Tab. 2, it was possible to see that the mathematical modeling did a good representation of the monthly clarity indexes, predicting values

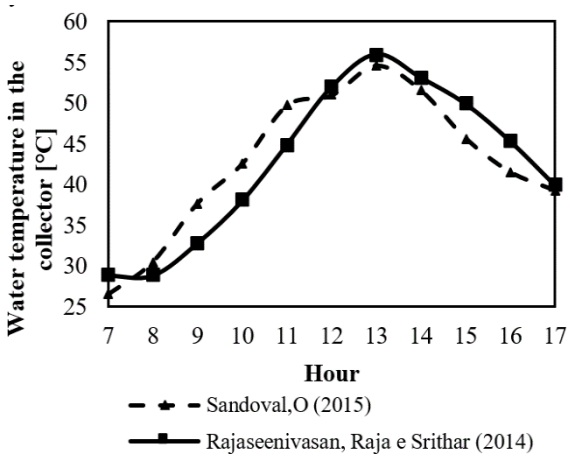

Figure 5. Comparison of how the temperature of the water inside the simulated collector varies according to the hour.

Table 2. Simulated collector's parameters.

Month	K_T Solarimetric Atlas (Cemig, 2011)	K_T SUNDATA (Censolar, 1993)	K_T simulated (I/I_o)	%error
Jan	0.39	0.51	0.49	20.4/4.1
Feb	0.45	0.54	0.52	13.5/3.8
Mar	0.44	0.54	0.54	18.5/0.0
Apr	0.48	0.58	0.54	11.1/7.4
May	0.53	0.59	0.56	5.3/5.3
Jun	0.42	0.62	0.61	31.1/1.6
Jul	0.56	0.64	0.61	8.2/4.9
Aug	0.48	0.63	0.61	21.3/3.3
Sep	0.44	0.58	0.57	22.8/1.7
Oct	0.47	0.54	0.52	9.6/3.8
Nov	0.39	0.49	0.47	17.0/4.2
Dec	0.38	0.47	0.45	15.5/4.4

Table 3. Losses simulated.

Month	U_T [MJ/m²day]
Jan	6.22
Feb	6.46
Mar	5.57
Apr	6.56
May	6.31
Jun	5.78
Jul	5.44
Aug	5.46
Sep	7.44
Oct	5.85
Nov	4.59
Dec	4.21

really close to, and in one case equal to the ones found in the SUNDATA (Censolar, 1993) database. On the other hand, the average error was of 3,7% for the SUNDATA from Censolar (1993) and 14,5% when comparing to Cemig's Solarimetric Atlas (2011). Since ambient temperature reaches lower values during winter, the energy losses get considerably higher, because the heat transfer between the covering glass and the outside environment increases. That being said, the system needs not only the amount of energy to heat the water but also some extra in order to compensate for those losses (see Tab. 3).

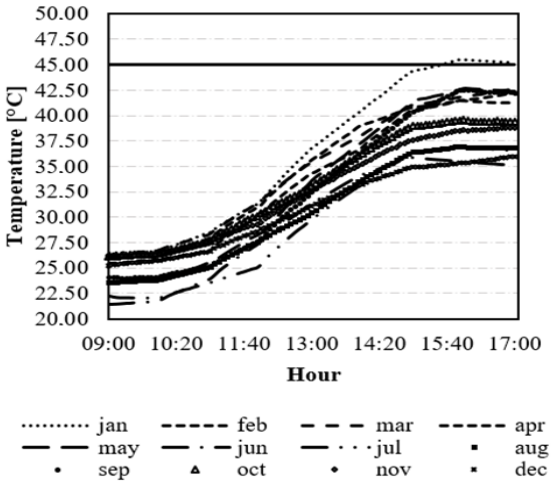

Figure 5. Temperature in the tank (200 l) during the simulation.

The hourly thermal behavior of the simulated collector is depicted in Fig. 6. The results of the simulation done on 17th of January were compared with the results obtained in researches in which real solar collectors were used with the intent of determining if the simulated collector behaved similarly of differently to the real solar collectors.

Comparing the results of the researches done by Rajaseenivasan, Raja and Srithar (2014) it was possible to determine that the simulated collector behaved very similarly to a real collector. The small differences can be explained by the difference in latitude between the cities of Belo Horizonte and

Tamil Nadu, India. Another difference is that the authors of that paper did their research on a horizontal solar collector, while the one in being studied here has an inclination of 36°.

It is possible to see that the biggest change in the temperature always occurred between the hours of 11 am and 3 pm (15h), since during this time of the day the collector was absorbing the biggest amount of solar radiation. It is also possible to notice that during the months of February, March, April, May and September, the temperature of the water reached 40 ºC, which can be considered as bathing suitable. The lowest temperatures occurred in the months of June, July, August and December, and did not go above 37°C. The lowest registered temperature occurred in the month of June, during which water got to a maximum of 35°C.

CONCLUSIONS

The losses of solar energy are mostly due to the collector's inclination and the low ambient temperatures in Belo Horizonte during some months of the year. According to this research, using the inclination in a correct manner allows for greater energy collected in the months when it is more needed, as is the case during winter.

The experimental results showed that, by simulating the historical solar data on the city of Belo Horizonte, January stands out from the other months because during this month there is no need for using any support mechanism, since with the use of alternative energy alone water is able to reach temperatures above 45°C.

The water temperature in the months of February, March, April, May and September can be considered as a temperature suited for human bathing and comfort, since in these months the temperature was kept between 40°C and 43°C, leading to the conclusion that solar energy is a type of clean energy that should be further explored.

ACKNOWLEDGEMENTS

The authors of this paper would like to thank Maxtemper company (www.maxtemper.com.br) and the Conselho Nacional de Desenvolvimento Científico e Tecnológico (CNPq), without which this research would not have been possible..

REFERENCES

ADEME, 2009, Energy Efficiency Trends and Policies in the Household & Tertiary Sectors in the EU 27, Agence de l'Environnement et la Maitrise de l'Energie, the ODYSSEE/MURE project.

Cooper, P. I., 1969, The Absorption of Radiation in Solar Stills, Solar Energy, Vol. 12, No. 3, pp. 333-346.

Dos Santos, M. J., dos Santos, M. A., Salvador, E., dos Santos, G. C., Siqueira, M. C., David, R. M., Ficara, R., and Rosito, L. H., 2011, Solar Heating Systems Evaluation in Low-Income Households, in: *XXI SNPTEE National Seminar on Production and Electricity Transmission*, Florianópolis, SC. Brasil.

Duffie, J. A., and Beckman, W. A., 2013, *Solar Engineering of Thermal Processes*, John Wiley & Sons, Inc.

Erbs, D. G., Klein, S. A., and Duffie, J. A., 1982, Estimation of the Diffuse Radiation Fraction for Hourly, Daily and Monthly-Average Global Radiation, Solar Energy, Vol. 28, No. 4, pp. 293-302.

Ibrahim, O., Fardoun, F., Younes, R., and Louahlia-Gualous H., 2014, Review of Water-Heating Systems: General Selection Approach Based on Energy and Environmental Aspects, Building and Environment, Vol. 72, pp. 259-286.

Levine, M., Ürge-Vorsatz, D., Blok, K., Geng, L., Harvey, D., Lang, S., Levermore, G., Mongameli Mehlwana, A., Mirasgedis, S., Novikova, A., Rilling, J., and Yoshino, H., 2007, Residential and Commercial Buildings. in: *Climate Change 2007: Mitigation. Contribution of Working Group III to the Fourth Assessment Report of the Intergovernmental Panel on Climate Change*, Cambridge University Press, Cambridge, United Kingdom.

Liu, B. Y. H., and Jordan, R. C., 1960, The Interrelationship and Characteristic Distribution of Direct, Diffuse and Total Solar Radiation, Solar Energy, Vol. 4, No. 3, pp. 1-19.

Pettit, R. B., and Sowell, R. R., 1976, Solar Absorptance and Emittance Properties of Several Solar Coatings, Journal of Vacuum Science & Technology, Vol. 13, No. 2, pp. 596-602.

Rajaseenivasan, T., Raja, P., and Srithar, K., 2014, An Experimental Investigation on a Solar Still with an Integrated Flat Plate Collector, Desalination, Vol. 347, pp. 131-137.

Sandoval, O. R., 2015, Development of a Solar Collector Simulator for Reproducing the Operating Conditions of a Heat Pump for Domestic Water Heating, Master Thesis, Universidade Federal de Minas Gerais, Belo Horizonte, MG. *(in Portuguese)*

Sandoval, O. R., dos Santos, R. M., Porto, M. P., Maia, A. A. T., and Koury, R. N. N., 2014, Comparison Experimental Between a Conventional and a Solar Evaporator of a Heat Pump Supporting a Solar Collector, in: V Brazilian Congress of Solar Energy, Recife, PE, Brazil. *(in Portuguese)*

Siegel, R., and Howell, J. R., 2002, *Thermal Radiation Heat Transfer*, 4nd. New York: CRC press.

Tabor, H., Bull., 1959, Radiation, Convection and Conduction Coefficients in Solar Collectors, Res. Council Israel 6C, Solar Energy, Vol. 3, No. 3, pp. 64-64.

Zhou, N., McNeil, M. A., Fridley, D., Lin, J., Price, L., Can, S. R., Sathaye, J., and Levine, M., 2008, *Energy use in China: Sectoral Trends and Future Outlook*, Lawrence Berkeley National Laboratory.